vation by catastrophic floods (*29*). After this initial flood, possible later flows would have been smaller discharges of Eridania lake subbasin A (Fig. 1A).

References and Notes

1. N. A. Cabrol, E. A. Grin, *Icarus* **142**, 160 (1999).
2. W. K. Hartmann, G. Neukum, *Space Sci. Rev.* **96**, 165 (2001).
3. R. P. Irwin III, A. D. Howard, *J. Geophys. Res.*, in press.
4. J. A. Grant, *Geology* **28**, 223 (2000).
5. R. D. Forsythe, C. R. Blackwelder, *J. Geophys. Res.* **103**, 31421 (1998).
6. T. J. Parker, S. M. Clifford, W. B. Banerdt, *Lunar Planet. Sci. Conf.* **31**, 2033 (2000).
7. T. J. Parker, R. S. Saunders, D. M. Schneeberger, *Icarus* **82**, 111 (1989).
8. J. W. Head III *et al.*, *Science* **286**, 2134 (1999).
9. D. E. Wilhelms, R. J. Baldwin, *Proc. Lunar Planet. Sci. Conf.* **19**, 355 (1989).
10. R. P. Sharp, M. C. Malin, *Geol. Soc. Am. Bull.* **86**, 593 (1975).
11. N. A. Cabrol, E. A. Grin, R. Landheim, *Icarus* **132**, 362 (1998).
12. N. A. Cabrol, E. A. Grin, G. Dawidowicz, *Icarus* **125**, 455 (1997).
13. D. E. Smith *et al.*, *J. Geophys. Res.* **106**, 23689 (2001).
14. G. D. Thornhill *et al.*, *J. Geophys. Res.* **98**, 23581 (1993).
15. N. A. Cabrol, E. A. Grin, G. Dawidowicz, *Icarus* **123**, 269 (1996).
16. J. E. O'Connor, *Geol. Soc. Am. Spec. Pap. 274* (1993).
17. N. A. Cabrol, E. A. Grin, R. Landheim, R. O. Kuzmin, R. Greeley, *Icarus* **133**, 98 (1998).
18. M. H. Carr, *Water on Mars* (Oxford Univ. Press, New York, 1996).
19. D. H. Scott, K. L. Tanaka, *U.S. Geol. Surv. Misc. Invest. Ser. Map I-1802-A* (1986).
20. R. Greeley, J. E. Guest, *U.S. Geol. Surv. Misc. Invest. Ser. Map I-1802-B* (1987).
21. R. A. Craddock, T. A. Maxwell, A. D. Howard, *J. Geophys. Res.* **102**, 13321 (1997).
22. A. D. Howard, *Eos* **81** (fall meet. suppl.), abstract P62C-06 (2000).
23. M. C. Malin, K. S. Edgett, *Science* **288**, 2330 (2000).
24. L. S. Manent, F. El-Baz, *Earth Moon Planets* **34**, 149 (1986).
25. H. V. Frey, K. M. Shockey, J. H. Roark, E. L. Frey, S. E. H. Sakimoto, 2001 GSA Annual Meeting, Boston, MA, 5 to 8 November 2001 (abstract 25358).
26. K. L. Tanaka, *J. Geophys. Res.* **91**, E139 (1986).
27. M. H. Carr, *J. Geophys. Res.* **84**, 2995 (1979).
28. P. D. Komar, *Icarus* **42**, 317 (1980).
29. B. L. Carter, H. Frey, S. E. H. Sakimoto, J. Roark, *Lunar Planet. Sci. Conf.* **32**, 2042 (2001).

30. Supported by NASA grants NAG5-3932 and NAG5-9817.

2 February 2002; accepted 3 May 2002

The Mass Disruption of Oort Cloud Comets

Harold F. Levison,[1]* Alessandro Morbidelli,[2] Luke Dones,[1] Robert Jedicke,[3] Paul A. Wiegert,[4] William F. Bottke Jr.[1]

We have calculated the number of dormant, nearly isotropic Oort cloud comets in the solar system by (i) combining orbital distribution models with statistical models of dormant comet discoveries by well-defined surveys and (ii) comparing the model results to observations of a population of dormant comets. Dynamical models that assume that comets are not destroyed predict that we should have discovered ~100 times more dormant nearly isotropic comets than are actually seen. Thus, as comets evolve inward from the Oort cloud, the majority of them must physically disrupt.

It has been over half a century since Jan Oort first argued that a roughly spherical cloud of comets, which extends to heliocentric distances larger than 100,000 astronomical units (AU), surrounds the solar system (*1*). This structure, which is now known as the Oort cloud, is currently feeding comets into the inner solar system (with perihelion distances, q, of less than 3 AU) at a rate of about 12 comets per year with an active comet absolute magnitude, H_{10}, <10.9 (*2*, *3*). These comets as a whole are known as nearly isotropic comets (NICs) (*4*). NICs can be divided into the following two subpopulations, based on their dynamical histories (*5*): (i) dynamically new NICs, which are on their first pass through the system and typically have semi-major axes, a, greater than ~10,000 AU, and (ii) returning NICs, which have previously passed through the inner solar system and typically have $a \leq 10{,}000$ AU.

One unsolved problem is that models of the orbital evolution of new NICs into returning NICs consistently predict many times more returning comets than are observed (*2*, *6*). This so-called "fading problem" cannot be due to previously unmodeled dynamical effects (*2*) and thus must be due to the physical evolution of the comets' activity (*7*). An important issue, therefore, is to determine the fate of the missing comets; either they become extinct or dormant (*8*), or they disintegrate entirely (*9*, *10*). Here, we try to distinguish between these two possible outcomes by comparing model results to observations of dormant comets.

Large ground-based surveys have discovered 11 asteroidal objects, as of 3 December 2001, that are on orbits consistent with active NICs with $q < 3$ AU (Table 1) (*11*) [see supporting online material (SOM)]. These 11 objects represent just a small fraction of the total population of dormant NICs, because ground-based surveys suffer from unavoidable observational biases (*12*). Thus, the main purpose of the work presented here is to estimate the total number of dormant NICs based on the available data. We accomplish this by the following steps: (i) we use numerical simulations of cometary dynamics to produce a set of fictitious dormant NICs, (ii) we run these fictitious NICs through a near-Earth object (NEO) survey simulator to determine which ones would be discovered, and (iii) we compare the results of (ii) to observations of the known dormant NICs to estimate the total number and orbital element distribution of the entire real dormant NIC population.

We determined the expected orbital element distribution for the dormant NICs from long-term dynamical simulations that track thousands of fictitious new comets entering the planetary system from the Oort cloud for the first time. The simulations calculate the dynamical evolution of these objects' orbits caused by the gravitational influence of the Sun, planets, and Milky Way Galaxy. The objects' trajectories are followed until they are either ejected from the solar system, hit a planet, or strike the Sun. From this, we can develop a steady-state distribution of NICs by assuming that the influx rate of dynamically new comets is constant with time.

We used simulations that were performed elsewhere (*2*, *13*). Because of differing computational challenges, these simulations have

Table 1. Known dormant NICs.

Asteroid Desig.	a (AU)	e	i (Deg)	q (AU)	H
(15504) 1999 RG_{33}	9.4	0.77	35	2.1	12.1
2000 DG_8	10.8	0.79	129	2.2	12.8
(5335) Damocles	11.8	0.87	62	1.6	13.3
2001 OG_{108}	13.3	0.93	80	1.0	13.0
1998 WU_{24}	15.2	0.91	43	1.4	15.0
1999 XS_{35}	18.0	0.95	19	0.95	17.2
(20461) 1999 LD_{31}	24.0	0.90	160	2.4	13.8
2000 HE_{46}	24.0	0.90	158	2.4	14.6
1997 MD_{10}	26.7	0.94	59	1.5	16.0
2000 AB_{229}*	52.5	0.96	69	2.3	14.0
1996 PW*	287	0.99	30	2.5	14.0

The columns are: Desig., designation; a, semi-major axis; e, eccentricity; i, inclination; q, perihelion distance; and H, Absolute Magnitude. See text for definitions. *All are type HTC, except the last two, which are ERCs.

[1]Southwest Research Institute, 1050 Walnut Street, Suite 426, Boulder, CO 80302, USA. [2]Observatoire de la Cote d'Azur, B. P. 4229, 06034 Nice Cedex 4, France. [3]Lunar and Planetary Laboratory, University of Arizona, Tucson, AZ 85721, USA. [4]Department of Physics, Queen's University, Kingston, Ontario K7L 3N6, Canada.

*To whom correspondence should be sent. E-mail: hal@gort.boulder.swri.edu

divided returning NICs into two subclasses: external returning comets (ERCs) with periods greater than 200 years, and Halley-type comets (HTCs) with orbital periods less than 200 years (*14*, *15*).

We used Wiegert and Tremaine's model (*2*) to determine the orbital element distribution that dormant ERCs would have if there were no disruptions. We also adopted the standard form for the cumulative absolute magnitude, H, distribution of $N(<H) \propto 10^{\alpha H}$ (*16*–*18*), where N is the total number of objects brighter than H and α is the slope of the H distribution. We set $\alpha = 0.28$. This value of α is determined directly from our models of the HTCs, which are described below. It is much smaller (or the H distribution is much shallower) than is typically assumed. However, it is consistent with a recent observational study of active comets (*19*).

With the above distribution of ERCs, we then used a survey simulator described in (*20*) to determine which objects would be discovered by modern NEO surveys. The survey simulator discovered 1 out of every 22,000 dormant ERCs with $q < 3$ AU and $H < 18$ (*21*) in Wiegert and Tremaine's model (*2*). This result, combined with the fact that only 2 dormant ERCs actually have been discovered thus far (Table 1) (also see SOM), implies that there are a total of 44,000 ± 31,000 dormant ERCs that are brighter than $H = 18$ and have a $q < 3$ AU in the solar system (*22*).

The ERCs have orbital periods that are so long that it is traditional to express the population numbers in terms of the number of objects that pass through perihelion per year. Based on the two objects thus far discovered and the mean inverse orbital period of objects in Wiegert and Tremaine's model (*2*), we estimate that there should be 3.9 ± 2.7 dormant ERCs with $H < 18$ and $q < 3$ AU passing perihelion per year. Assuming no disruptions, Wiegert and Tremaine's model predicts that there should be ~400 dormant ERCs with $q < 3$ AU passing perihelion per year (see SOM). The discrepancy between our estimate based on observing dormant NICs and the one based on dynamics alone implies that, when a comet becomes inactive, it only has a ~3.9/400, or 1%, chance of becoming dormant. We can only conclude that the other ~99% of these objects must have disrupted.

To perform these calculations, we assumed a value of $\alpha = 0.28$. We must therefore estimate how this choice affects our result concerning the disruption of ERCs. Previous estimates of α have ranged from 0.28 to 0.53 (*23*). As we discussed above, if we assume that $\alpha = 0.28$, our survey simulator discovers 1/22,000 of the dormant ERCs with $H < 18$. If α were 0.53, our survey simulator would discover 1/43,000 of these objects, which is only a factor of 2 different from the $\alpha = 0.28$ result. Thus, changing α does not change our conclusion that ~99% of the inactive ERCs disrupt.

We now turn our attention to the HTCs. Levison *et al.* (*13*) studied the dynamical evolution of comets from the Oort cloud into HTC-like orbits (restricting themselves to HTCs with $q < 2.5$ AU). As with the ERCs, Levison *et al.* found a significant fading problem with the HTCs. In particular, Levison *et al.*'s models predict that there should be more than 15,000 active HTCs in the solar system, whereas the debiased estimate of active HTCs based on the observed population would suggest that there are only 50 (*13*). Thus, they concluded that ≥99% of these comets disappeared.

To determine whether HTCs become dormant or disrupt, we compare a model of dormant HTC discoveries (i.e., we take the results of dynamical models with no disruption and run them through our survey simulator) to actual discoveries. If we adopt Levison *et al.*'s models unaltered (see SOM), we are unable to construct models of the dormant HTC population that are consistent with observations (Fig. 1). Although the models produce reasonable inclination distributions (Fig. 1D), they fail to reproduce the observed semi-major axis distribution (Fig. 1C). In particular, the models predict a far larger number of dormant HTCs with $a < 10$ AU than has been observed.

One reason Levison *et al.*'s model fails could be that it does not adequately account for the fact that comets suffering a close encounter with the Sun are more likely to disrupt than are comets that have larger perihelion distances. Thus, we added a q-sensitive disruption law (*24*) to Levison *et al.*'s model and assumed that the absolute magnitude power law index is $\alpha = 0.28$ (as before). We then recalculated Levison *et al.*'s fitting procedures and determined the model that provides the best fit to both the active and dormant HTC populations (see SOM). This

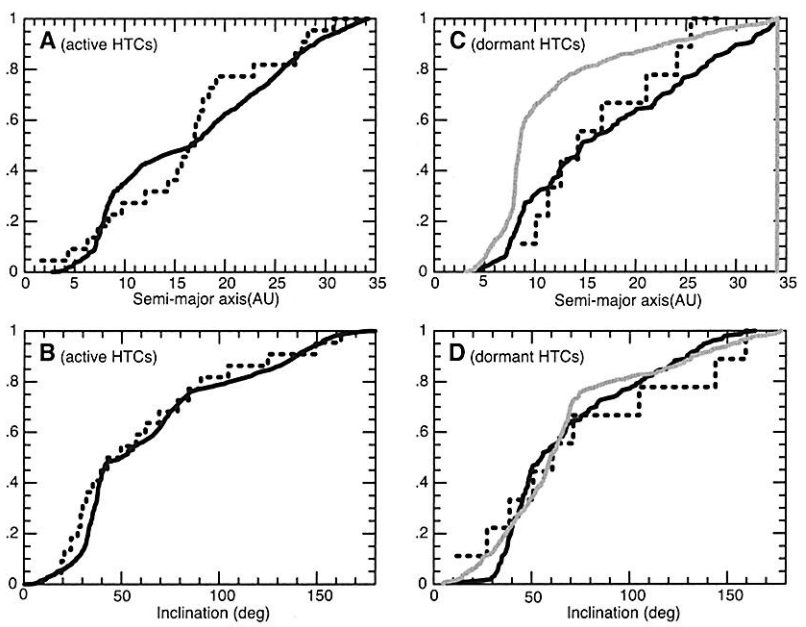

Fig. 1. The cumulative semi-major axis (*a*) distribution (**A** and **C**) and inclination distribution (**B** and **D**) for observed active HTCs (A) and (B) and dormant HTCs (C) and (D). The dotted curves represent the real objects observed in the solar system. The gray curves show the distributions of dormant comets as predicted by processing the unbiased best-fit dynamic model through our survey simulator [see (*13*) for the distribution of active comets]. The black curves show these distributions for our best-fit model.

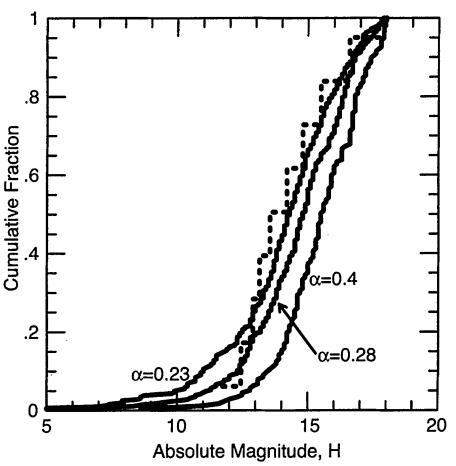

Fig. 2. The cumulative absolute magnitude (H) distribution of dormant HTCs discovered by NEO surveys. The dotted curve represents the real objects. The solid curves show the distribution predicted by our best-fit model for three different values of α (0.23, 0.28, and 0.4).

model shows good agreement with the observations (Fig. 1).

Up to this point, we have been assuming a value of α. We could not determine α for the ERC simulations because there are only two known dormant ERCs. There are enough known dormant HTCs (nine of them), however, to estimate α directly. The cumulative absolute magnitude distribution (*25*) for the observed dormant HTCs is clearly inconsistent with those detected by our survey simulator for values of α as large as 0.4 (Fig. 2). Indeed, the probability that the observed and modeled absolute magnitude distributions are drawn from the same parent distribution (fig. S2) shows that we can rule out any α larger than $\sim$0.35 and that the best fit is $\alpha = 0.23 \pm 0.04$ (1σ). We decided to adopt Weissman and Lowry's (*19*) value of 0.28 because it is consistent with our results and yet is based on a larger data set. The differences between models using $\alpha = 0.28$ and $\alpha = 0.23$ are small, and thus this choice will not measurably affect our results.

With $\alpha = 0.28$, the survey simulator discovers 1.1% of the dormant HTCs. Given that the NEO surveys have discovered 9 dormant HTCs (Table 1), we conclude that there are 780 ± 260 dormant HTCs in the solar system with $H < 18$ and $q < 2.5$ AU.

We can now compare our estimate of the number of dormant HTCs to what we would expect from dynamical models, assuming no disruption (*26*). Our model predicts that there should be 46,000 active and dormant HTCs with $q < 1.3$ AU, which implies $\sim$106,000 with $q < 2.5$ AU. Because dormant comets far outnumber active comets (*27*), we can conclude that $\sim$99% of ERCs disrupt before becoming HTCs. This percentage is similar to the fraction predicted for the ERCs alone.

Jupiter-family comets (JFCs) do not appear to disrupt at the same rate (*28*) as do the NICs. Bottke *et al.* (*29*) estimated the total number of dormant JFCs from the known population of NEOs, finding that there are 61 ± 43 dormant JFCs with $q < 1.3$ AU and $H < 18$. This number is consistent with estimates from dynamical simulations, assuming that all objects become dormant rather than disrupt [$\sim 60^{+40}_{-53}$% become dormant (*30*)]. Despite large uncertainties in this estimate, it is clear that a substantial fraction of JFCs must become dormant, and thus they behave differently from NICs (see SOM for additional arguments).

It is surprising that NICs and JFCs behave so differently, because they are thought to be composed of similar mixtures of ice and rock. Their different disruption behaviors could be primordial, reflecting the chemical or physical characteristics of their formation locations. Most Oort cloud comets are believed to have formed in the region of the giant planets (*1*, *31*), whereas JFCs are thought to have formed in the Kuiper belt beyond the giant planets (*32*–*34*). However, recent simulations of Oort cloud formation (*35*) suggest that $\sim$30% of the present-day Oort cloud originated in the Kuiper belt (although most of these objects left the Kuiper belt a long time ago). If these models are correct, then the different disruption behaviors cannot stem from primordial differences, because the fraction of NICs that originated in the Kuiper belt is far larger than the $\sim$1% that avoid disruption.

Alternatively, evolutionary processes could affect comets' susceptibility to disruption. For example, over long time scales, Kuiper belt comets could have lost more volatiles than did Oort cloud comets because Kuiper belt comets have been stored at closer heliocentric distances and thus higher temperatures. Kuiper belt objects could be more porous, and thus less susceptible to disruption resulting from volatile pressure buildup, due to a relatively violent collisional environment (*36*). Finally, the dynamical pathways that NICs and JFCs take on their way into the inner solar system might lead to different thermal histories for the two populations. In one orbital period, most NICs evolve from distant orbits (with perihelia outside the planetary region) to orbits that closely approach the Sun. On the other hand, objects from the Kuiper belt slowly move through the planetary region, taking $\sim$10 million years to evolve onto orbits with $q < 2.5$ AU (*33*). It has been argued previously (*37*) that different thermal histories could lead to different disruption rates, so perhaps NICs disrupt because of strong thermal gradients or volatile pressure buildup, whereas JFCs survive because they are warmed more slowly.

References and Notes

1. J. H. Oort, *Bull. Astron. Inst. Neth.* **11**, 91 (1950).
2. P. Wiegert, S. Tremaine, *Icarus* **137**, 84 (1999).
3. H_{10} is a distance-independent measure of the brightness of active comets that includes the coma.
4. We use the notation of (*14*). An NIC is defined as an object that has a Tisserand parameter, T, with respect to Jupiter, of less than 2. The encounter velocity with Jupiter is $v_j\sqrt{3 - T}$, where v_j is the mean orbital velocity of Jupiter around the Sun. NICs typically have semi-major axes greater than that of Jupiter.
5. On their first trip through the inner solar system, NICs have semi-major axes, a, larger than $\sim$10,000 AU. The large a's result from the dynamics of the Oort cloud itself. Oort cloud comets are brought into the planetary region by the gravitational effects of the Galaxy, which act like a tide. The tide grows larger as a comet moves farther from the Sun. Objects initially on orbits with $a < 10{,}000$ AU rarely make it directly into the inner solar system because they first gravitationally encounter a giant planet [see (*31*, *38*) for a more complete discussion]. However, beyond $\sim$10,000 AU, the tides are strong enough that a comet can effectively jump over the jovian planet region (i.e., the comet's perihelion distance, q, can evolve from $\geq$10 to $\leq$3 AU in just one orbital period). Thus, it can arrive in the inner solar system without being measurably perturbed by a giant planet. Once comets are in the inner planetary system for the first time, gravitational interactions with the giant planets can then either eject them from the solar system entirely or markedly alter their semi-major axes from $a > 10{,}000$ AU to much smaller values. (*1*, *9*, *39*). Thus, comets that have made more than one passage through the planetary system, which are called returning comets, typically have smaller semi-major axes than do those on their first passage.
6. P. R. Weissman, *Astron. Astrophys.* **85**, 191 (1980).
7. NICs are the brightest and most active during their first few passages through the planetary system and then disappear before subsequent passages [see (*2*) and references therein].
8. A comet becomes extinct if it loses all its volatiles. It becomes dormant if, as a result of its passages through the planetary system, a lag deposit of inert material builds up over its entire surface (*40*, *41*). Such mantles have been observed to cover large fractions of the two comets that have been imaged in detail by spacecraft flybys [i.e., 1P/Halley (*42*), which is an NIC, and 19P/Borrelly (*43*)]. A dormant comet can become active again if its mantle is disturbed. In this paper, we do not take this reactivation into account. We also do not distinguish between dormant and extinct comets and we henceforth refer to both states as dormant.
9. P. R. Weissman, in *Dynamics of the Solar System, IAU Symposium 81*, R. L. Duncombe, Ed. (Reidel, Dordrecht, Netherlands, 1979), pp. 277–282.
10. Such events are known to happen, as illustrated by the spectacular disruption of comet C/1999 S4 (LINEAR) (*44*). See http://oposite.stsci.edu/pubinfo/PR/2000/27/ for images taken with the Hubble Space Telescope.
11. Dormant comets will look like asteroids because they lack, by definition, any cometary activity. Thus, they are classified as asteroids by the International Astronomical Union and are given asteroid designations. However, physically they still are dormant comets.
12. R. Jedicke, J. Larsen, T. Spahr, in *Asteroids III*, W. F. Bottke, A. Cellino, P. Paolicchi, R. Binzel, Eds., (Univ. Arizona Press, Tucson, AZ, in press).
13. H. F. Levison, L. Dones, M. J. Duncan, *Astron. J.* **121**, 2253 (2001).
14. H. F. Levison, in *Completing the Inventory of the Solar System*, T. W. Rettig, J. M. Hahn, Eds. (Astronomical Society of the Pacific, San Francisco, 1996), pp. 173–192.
15. HTCs have small enough semi-major axes that planetary–mean motion resonances can play a role in their evolution (*45*). These resonances are unimportant for external returning comets or ERCs. Hence, external implies that the comet is beyond the region where resonances are important. For our purposes, this distinction is made for historical and numerical reasons. As comets evolve out of the Oort cloud, a larger fraction become ERCs than become HTCs, so the study of these two NIC subclasses requires different numerical techniques. Wiegert and Tremaine (*2*) studied only ERCs, whereas Levison *et al.* (*13*) studied the HTCs alone. We treat these two studies separately.
16. E. Everhart, *Astron. J.* **72**, 1002 (1967).
17. D. W. Hughes, *Mon. Not. R. Astron. Soc.* **326**, 515 (2001).
18. This absolute magnitude distribution is equivalent to a differential size distribution that is also a power law of the form $dN/dD \propto D^{-(5\alpha + 1)}$, where D is an object's diameter. A collisional equilibrium corresponds to $\alpha = 0.5$.
19. P. R. Weissman, S. C. Lowry, *Bull. Am. Astron. Soc.* **33**, 1094 (2001).
20. R. Jedicke, A. Morbidelli, T. Spahr, J.-M. Petit, W. Bottke, *Icarus*, in press.
21. Our brightness limit is somewhat arbitrary. We chose it because it is the next integer fainter than the faintest object in Table 1, which has $H = 17.2$. Assuming an albedo of 2% (*46*), an $H = 18$ object has a diameter of 2.4 km.
22. Our quoted error is 1σ. We calculated it assuming Poisson statistics using the two objects thus far discovered.
23. The classic measurement is by (*47*), who estimated α using the size distribution of craters on the Galilean satellites of Jupiter. More recent measurements using the observed magnitudes of comets far from the Sun are $\alpha = 0.53 \pm 0.05$ (*48*), 0.32 ± 0.02 (*49*), and

0.28 ± 0.03 (*19*). The measurements of α using cometary nuclei need to be viewed with caution, because they are observationally challenging, and so the measurements could have problems. For example, measurements of individual comets could have been performed when there was still some small amount of cometary activity—too small to resolve but large enough to affect the photometry. In addition, all objects studied in these surveys are bright active comets when observed near perihelion, which could introduce biases in the way they were selected. What is clearly needed is a population of dormant objects whose members were discovered in a systematic way. The data set studied here supplies us with such a population.

24. Levison *et al.* assume that active comets fade in brightness over many orbits after they reach $q < 2.5$ AU. However, they do not distinguish between close (say, $q \sim 0.5$ AU) and distant (say, $q \sim 2.5$ AU) passages. We believe, however, that closer perihelion passages lead to increased damage to comets. For this reason, we have added an additional disruption law to Levison *et al.*'s models. This simple law is designed to mimic the q dependence of fading, while making the fewest changes to the original Levison *et al.*'s models. If an object evolves onto an orbit with $q < 1$ AU, we assume that it has a 96% chance of disrupting before its next perihelion passage (see SOM). If the comet disrupts, it will not appear in either the active comet or dormant comet populations.
25. Fortunately, the *a–i* distribution (i.e., semi-major axis and inclination) of our models is not sensitive to α, so we can perform the absolute magnitude fitting procedure on our best-fit model alone. In particular, we do not need to perform a calculation that varies the four parameters from (*13*) and α, while fitting to *a*, *i*, and *H* simultaneously.
26. To do this comparison, we use arguments developed in (*13*) for relating the observed number of dynamically new comets per year to the total number of HTCs.
27. There are 22 known active HTCs with $q < 1.3$ AU (a limit set by observational biases), although not all HTCs with $q < 1.3$ AU have yet been discovered. We can predict the total number of active HTCs with our dynamical models. Our best-fit model for the HTCs predicts 84 active HTCs with $q < 1.3$ AU. This value, in turn, implies that there are 194 active HTCs with $q < 3$ AU.
28. JFCs are comets with Tisserand parameters $2 < T \leq 3$ [see (*4*, *14*)]. These objects are believed to arise in the Kuiper belt (*32*, *33*) or the scattered disk (*34*)—not in the Oort cloud.
29. W. F. Bottke Jr. *et al.*, *Icarus* **156**, 399 (2002).
30. From results given in (*48*), we estimate that there are 30^{+10}_{-5} active JFCs with $H < 18$ and $q < 1.3$ AU. From (*33*), for each active comet, there should be between 2.0 and 6.7 dormant comets, with a best-fit value of 3.5. This assumes no disruption. Thus, we estimate that the total number of dormant JFCs with $H < 18$ and $q < 1.3$ AU is $30 \times 3.5 = 105$, with a possible range of 50 to 268, if all inactive comets become dormant. Given Bottke's (*29*) estimate of dormant JFCs from the NEO surveys (61 with $H < 18$), our best estimate is that 61/105, or ~60%, of the JFCs become dormant, as opposed to ≤1% of the NICs. Formally, the fraction of JFCs that become dormant could be as small as 7% or as large as 100%. Even the lower limit is about an order of magnitude larger than our upper limit for the fraction of NICs that become dormant.
31. M. Duncan, T. Quinn, S. Tremaine, *Astron. J.* **94**, 1330 (1987).
32. ———, *Astrophys. J. Lett.* **328**, 69 (1988).
33. H. F. Levison, M. J. Duncan, *Icarus* **127**, 13 (1997).
34. M. J. Duncan, H. F. Levison, *Science* **276**, 1670 (1997)
35. L. Dones, H. F. Levison, M. J. Duncan, P. R. Weissman, *Am. Astron. Soc. Div. Dynamical Astron. Meeting* **32**, 1103 (2001).
36. The Kuiper belt is currently collisionally active (*50*), whereas the Oort cloud is not.
37. M. Bailey, *Mon. Not. R. Astron. Soc.* **221**, 247 (1984).
38. J. G. Hills, *Astron. J.* **86**, 1730 (1981).
39. F. L. Whipple, *Astron. J.* **67**, 1 (1962).
40. G. D. Brin, D. A. Mendis, *Astrophys. J.* **229**, 402 (1979).
41. D. Prialnik, A. Bar-Nun, *Icarus* **74**, 272 (1988).
42. H. U. Keller *et al.*, *Nature* **321**, 320 (1986).
43. L. Soderblom *et al.*, *Science* **296**, 1087 (2002).
44. H. Boehnhardt, *Science* **292**, 1307 (2001).
45. J. Chambers, *Icarus* **125**, 32 (1997).
46. Y. R. Fernández, D. C. Jewitt, S. S. Sheppard, *Astrophys. J. Lett.* **553**, L197 (2001).
47. E. M. Shoemaker, R. F. Wolfe, in *Satellites of Jupiter*, D. Morrison, Ed. (Univ. Arizona Press, Tucson, AZ, 1982), pp. 277–339.
48. J. A. Fernández, G. Tancredi, H. Rickman, J. Licandro, *Astron. Astrophys.* **352**, 327 (1999).
49. S. C. Lowry, thesis, Queen's University, Belfast, UK (2001).
50. S. A. Stern, J. E. Colwell, *Astrophy. J.* **490**, 879 (1997).
51. We thank M. Duncan, S. A. Stern, and P. Weissman for useful discussions and comments on an early draft of this paper; and M. Bailey for useful comments on this manuscript. H.L., W.B., and L.D. acknowledge support from NASA's Planetary Geology and Geophysics (NAG5-9479, NAG5-10331, NAG5-9141), Origins of Solar Systems (NAG5-10661), NEO-Observations (NAG5-9951), and Mars-Data Analysis (NAG5-10603) programs. A.M. was subsidized by European Space Agency contract 14018/2000/F/TB. Travel support provided by grants from NATO and NSF/Centre National de la Recherche Scientifique. Observations by Spacewatch and research by R.J. supported by grants from NASA (NAG5-7854, NAG5-10447, NAG5-7533), the Air Force Office of Scientific Research (F49620-00-1-0126), the David and Lucile Packard Foundation, the Steven and Michele Kirsch Foundation, the Paul G. Allen Charitable Foundation, and other contributors.

Supporting Online Material

www.sciencemag.org/cgi/content/full/296/5576/2212/DC1
Materials and Methods
Figs. S1 and S2
References and Notes

25 January 2002; accepted 3 April 2002

Identification of Signal Peptide Peptidase, a Presenilin-Type Aspartic Protease

Andreas Weihofen,[1] Kathleen Binns,[2] Marius K. Lemberg,[1] Keith Ashman,[2] Bruno Martoglio[1]*

Signal peptide peptidase (SPP) catalyzes intramembrane proteolysis of some signal peptides after they have been cleaved from a preprotein. In humans, SPP activity is required to generate signal sequence–derived human lymphocyte antigen–E epitopes that are recognized by the immune system, and to process hepatitis C virus core protein. We have identified human SPP as a polytopic membrane protein with sequence motifs characteristic of the presenilin-type aspartic proteases. SPP and potential eukaryotic homologs may represent another family of aspartic proteases that promote intramembrane proteolysis to release biologically important peptides.

The discovery of intramembrane proteolysis has revealed alternative pathways in cell signaling, cell regulation, and protein processing (*1*). Dormant, membrane-bound transcription factors, like sterol regulatory element–binding protein (*1*), activating transcription factor–6 (*2*), and NOTCH (*3*), or the growth factor Spitz in *Drosophila* (*4*), are activated and liberated in regulated processes that culminate in proteolytic cleavage within their membrane anchor. Similarly, β-amyloid (Aβ) peptides, which are believed to be the main toxic component in Alzheimer's disease, are generated from membrane-anchored β-amyloid precursor protein (β-APP) (*5*). The critical cleavage in the membrane anchor of β-APP is thought to be catalyzed by the aspartic protease presenilin (*6*).

Processing of signal peptides by an SPP is related to protein cleavage by presenilin. Both proteases cleave their substrates within the center of a transmembrane region (*6*, *7*). The discovery of posttargeting functions of signal peptides, which are required primarily for the biosynthesis of secretory and membrane proteins, has pointed to a central role for SPP activity (*8*). Generation of cell surface histocompatibility antigen (HLA)–E epitopes in humans requires processing of signal peptides by SPP (*9*). HLA-E epitopes originate from the signal sequence of polymorphic major histocompatibility complex (MHC) class I molecules and report biosynthesis of these molecules to the immune system (*10*). SPP activity is also required for processing hepatitis C virus polyprotein and hence is exploited by the pathogen to produce viral components (*11*). It is thought that SPP promotes the liberation of functional signal peptide fragments from the endoplasmic reticulum (ER) membrane (*8*).

To identify human SPP, we synthesized a ligand affinity probe based on the SPP inhibitor $(Z\text{-}LL)_2$–ketone, which is thought to re-

[1]Institute of Biochemistry, Swiss Federal Institute of Technology (ETH), ETH-Hoenggerberg, 8093 Zürich, Switzerland. [2]Samuel Lunenfeld Institute, Proteomics, 600 University Avenue, Toronto, Ontario M5G 1X5, Canada.

*To whom correspondence should be addressed. E-mail: bruno.martoglio@bc.biol.ethz.ch